# Properties and Application of Double-Walled Carbon Nanotubes Sorted by Outer-Wall Electronic Type

**Alexander A. Green[†] and Mark C. Hersam[*]**

Department of Materials Science and Engineering and Department of Chemistry, Northwestern University, Evanston, Illinois 60208-3108, United States

[†] Present address: Wyss Institute for Biologically Inspired Engineering, Harvard University, Boston, Massachusetts 02215

**ABSTRACT** Double-walled carbon nanotubes (DWNTs) can adopt four distinct permutations arising from the electronic type (metallic or semiconducting) of their inner and outer walls. This polydispersity limits the utility of DWNTs in applications such as thin film electronics. We demonstrate that density gradient ultracentrifugation can be employed to address this source of heterogeneity by producing DWNTs with well-defined outer-wall electronic types. Optical absorption measurements of sorted DWNTs reveal outer-wall purities of 96% and 98% for sorted semiconducting and metallic samples, respectively. Electrical characterization of semiconducting and metallic outer-wall DWNTs in thin film transistors directly confirms the efficacy of these separations, with semiconducting DWNT devices yielding on/off ratios 2 orders of magnitude higher than comparable metallic DWNT devices.

**KEYWORDS:** carbon nanotube · double · density gradient ultracentrifugation · separation · sorting · purification · transistor

Double-walled carbon nanotubes (DWNTs) are intriguing materials that exhibit properties intermediate between those of single-walled carbon nanotubes (SWNTs) and multiwalled carbon nanotubes (MWNTs). These carbon nanomaterials formed from two concentric cylinders of graphene can be routinely synthesized with outer-wall diameters below 2 nm, and they exhibit band gaps that are sufficiently large for use in field-effect transistors.[1−3] At the same time, DWNTs can offer several of the beneficial properties typically observed for MWNTs, such as improved lifetimes and current densities for field emission[4] and high stability under aggressive chemical,[5] mechanical,[6] and thermal treatments.[7] Recent efforts to develop outer-wall selective functionalization schemes[5] also point to the use of DWNTs as core−shell systems having pristine carbon nanotube cores and chemically functionalized nanotube shells for use as imaging and therapeutic agents in biological systems.

Attempts to investigate and exploit the beneficial attributes of DWNTs have been hindered by their polydispersity. For example, DWNTs are synthesized in heterogeneous mixtures containing SWNTs and MWNTs having three or more walls.[8−10] Beyond these variations in wall number, both DWNT walls exhibit the same modes of polydispersity in diameter and electronic type observed for SWNTs.[11] Even though the condition that the inner and outer walls of DWNTs typically differ by ~0.34 nm (*i.e.*, the interlayer spacing of graphite) reduces the degree of structural variability, DWNTs remain a considerably more complicated system in which to confront the polydispersity problem compared to SWNTs. Previously, we have shown that density gradient ultracentrifugation[12] (DGU) can be used to isolate DWNTs from impurity single-walled and multiwalled carbon nanotubes.[6] In a DGU separation, polydisperse input nanomaterials, such as carbon nanotubes[13] and graphene,[14] are driven by high centripetal forces to isopycnic positions in a density gradient where their buoyant density matches that of the surrounding medium. Since the buoyant density of surfactant-encapsulated nanomaterials depends strongly on their physical and electronic structure, DGU separations improve nanomaterial homogeneity. In the case of DWNTs, this approach can exploit the density contributions of inner carbon nanotube walls to achieve separation by wall number. Since our initial report,[6] DGU-based purification of DWNTs has been reproduced by other groups,[6,15,16] including a recent study by Huh and colleagues which described partial enrichment of DWNTs by their electronic type.[17]

Herein, we report nearly complete isolation of DWNTs having metallic or semiconducting outer walls using cosurfactant DGU. Optical absorption and Raman spectroscopy are used to validate electronic type enrichment with the former indicating purities

[*] Address correspondence to m-hersam@northwestern.edu.

Received for review November 30, 2010 and accepted January 20, 2011.

**Published online January 28, 2011**
**10.1021/nn103263b**

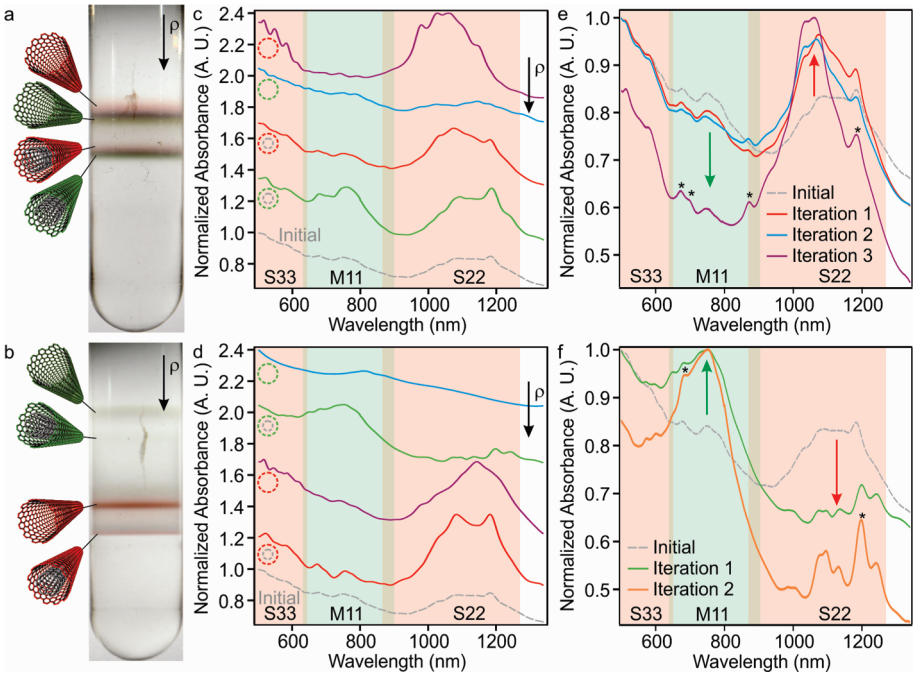


**Figure 1. Separation of DWNTs by outer-wall electronic type. (a,b) Photographs of centrifuge tubes following DGU separations of SWNT/DWNT mixtures targeted for semiconducting (a) and metallic (b) DWNTs. Four bands of carbon nanotubes are identified in each separation and correspond to semiconducting and metallic SWNTs and semiconducting and metallic outer-wall DWNTs. (c,d) Optical absorbance spectra obtained from carbon nanotubes isolated during the first iteration separations targeting semiconducting (c) and metallic (d) DWNTs. Metallic DWNTs, semiconducting DWNTs, metallic SWNTs, semiconducting SWNTs, and the coarsely enriched input DWNT material are shown as red, green, purple, blue, and dashed gray curves, respectively. Spectra are offset for clarity. (e,f) Optical absorbance spectra obtained during successive DGU iterations to produce semiconducting (e) and metallic (f) DWNTs. Asterisks mark absorption peaks attributed to inner DWNT wall transitions. S*ii* (M*ii*) label *i*th order semiconducting (metallic) optical transitions of the SWNTs and outer walls of DWNTs. Wavelength regions associated with semiconducting and metallic SWNT and outer-wall DWNT transitions are shaded red and green, respectively.**

of 96% and 98% for semiconducting and metallic DWNTs, respectively. In agreement with previous reports,[6,15] only weak photoluminescence is observed from the inner nanotubes of sorted DWNT suspensions as a result of nonradiative exciton quenching by the outer walls. Electrical measurements of thin film transistors (TFTs) produced from networks of semiconducting and metallic DWNTs directly confirm the efficacy of electronic type enrichment, with semiconducting DWNT devices displaying on/off ratios greater than 1000, which is more than 2 orders of magnitude higher than comparable metallic DWNT devices.

## RESULTS AND DISCUSSION

DWNTs having outer walls of either semiconducting or metallic electronic type were produced using a multistep DGU separation strategy (see Methods and Supporting Information). The starting material for these separations was purified double-walled carbon nanotubes (Unidym, Inc.) specified to consist of ~60% double-walled species. Prior to high resolution DGU sorting, this input material was dispersed in sodium cholate (SC) and run through a density gradient separation designed to achieve coarse separation of the carbon nanotubes by wall number. This stage employed a gradient containing SC alone for efficient diameter separation, and the nanotubes were placed at the top of the density gradient region to encourage them to sediment downward in the centrifuge tube to their isopycnic points. As a result, most of the buoyant small and large diameter SWNT species present in the starting material were captured in the upper regions of the density gradient thereby allowing the denser DWNT-enriched material to be harvested from the regions below. The coarsely separated DWNT material was characterized by optical absorbance spectroscopy, which revealed clear semiconducting and metallic absorption peaks at the energies expected for outer-wall carbon nanotubes having diameters of *ca.* 1.5−1.6 nm (see dashed gray curve in Figure 1c). This DWNT-enriched material was then incorporated into cosurfactant gradients containing SC and sodium dodecyl sulfate (SDS) similar to those previously used for the separation of large diameter SWNTs by electronic type.[13,18,19]

Cosurfactant density gradients containing a 1:4 SDS/SC ratio and a 3:2 SDS/SC ratio were employed for optimal isolation of semiconducting and metallic species, respectively. For semiconductor-targeted 1:4 SDS/SC ratio experiments, SWNT separations lead to a pair of closely spaced bands inside the density gradient whose positions, and hence buoyant density, do not

vary strongly with SWNT diameter. The upper band in these separations contains highly enriched semiconducting SWNTs, and the lower band contains ~67% metallic SWNTs.[13] Given the insensitivity to SWNT diameter of these cosurfactant separations, we expected that analogous experiments using partially enriched DWNT material would lead to efficient separation of the carbon nanotubes by wall number, with the DWNTs reaching equilibrium at lower regions of the gradient due to the density contribution of their inner walls. Figure 1a displays a centrifuge tube following a proof-of-concept separation using a starting carbon nanotube solution containing both SWNTs and DWNTs. Clearly visible are two pairs of colored nanotube bands arising from the single- and double-walled species that are simultaneously separated by electronic type.

In 3:2 SDS/SC DGU separations, enrichment of metallic SWNTs occurs concomitantly with isolation by diameter and leads to the population of the more buoyant regions of the density gradient with distinct bands of diameter-resolved metallic species.[18] The semiconducting SWNTs, on the other hand, are found in the densest portions of the gradient. As expected, band pairing is also observed for metal-targeted separations of the SWNT/DWNT mixture in a 3:2 SDS/SC ratio as shown in Figure 1b. A green band consisting of large diameter metallic SWNTs reaches equilibrium at the lowest buoyant density, followed by a faint band of metallic DWNTs a few millimeters below. Red bands consisting of semiconducting enriched carbon nanotubes can be observed in the denser regions of the gradient.

The coarsely enriched DWNT material obtained from the initial SC separation was then sorted using the above cosurfactant combinations inside density gradients in which the carbon nanotubes moved from dense to buoyant regions during the ultracentrifugation. Absorbance spectra acquired from the four principal bands of the semiconducting DWNT separation are shown in Figure 1c (see Supporting Information for additional absorbance spectra). The pair of bands obtained from the SWNT region exhibit signs of electronic type sorting. The semiconducting SWNT fraction has strongly suppressed first-order metallic transitions (M11) as expected (see Supporting Information, Figure S-1 for Kataura plot with DWNT transition wavelengths). The other SWNT fraction displays relatively weak absorption peaks compared to the absorbance background, possibly as a result of SWNTs with small average lengths[17,20] or significant defect levels in this fraction. Despite the attenuated absorption peaks from these SWNTs, the M11 transitions appear to be enhanced compared to the second-order semiconducting transitions (S22) and consequently suggest enrichment of metallic species. The absorbance spectra of the DWNT fractions show strong changes in the relative strengths of the M11 and S22 transitions of the outer-wall nanotubes, as expected for electronic type separated material. In addition, both fractions possess a characteristic absorption peak at ~1200 nm that doping studies (see below) indicate is due to the DWNT inner walls.

Absorbance spectra from the four principal bands of the metallic DWNT separation are shown in Figure 1d. As with the semiconducting-targeted separation, the semiconducting SWNT and both DWNT fractions display clear spectroscopic evidence of enrichment by electronic type due to changes in the strength of the M11 and S22 absorption peaks. The DWNT fractions also present the characteristic ~1200 nm transition arising from the inner walls. The metallic SWNT fraction exhibits suppression of S22 absorption as expected, yet it also possesses a smaller peak-to-background ratio compared to the other fractions.

Although the optical absorbance spectra of the metallic and semiconducting DWNTs suggest electronic type purities in excess of ~90%, these DWNT samples were iteratively separated in additional density gradients to enhance the degree of wall number and electronic type enrichment. High purity semiconducting outer-wall DWNTs (s-DWNTs) were obtained using two additional DGU separations. The first of these iterations was conducted in a 1:4 SDS/SC gradient and forced the nanotubes to move downward in the gradient from lower to higher densities. This step ensured that slowly sedimenting SWNTs that did not reach their isopycnic points during the previous iteration could be captured before they reached the banding position of the best semiconducting DWNTs. In the final iteration, the remaining metallic SWNTs and DWNTs present in the material were targeted in a 3:2 SDS/SC gradient in which the nanotubes moved from low to high densities in the gradient. Figure 1e presents the optical absorbance spectra of the material isolated from each of the above iterations. Over the three iterations, there are clear signs of improvement in degree of semiconducting DWNT purity as the S22 optical transitions increase in strength and the M11 transitions decrease in intensity. In addition, there is a ~25% decrease in background absorption strength between the second and third iterations (see Supporting Information, Figure S-2). The majority of this reduction is caused by the removal of the metallic SWNTs having low peak-to-background ratios.

The metallic outer-wall DWNTs (m-DWNTs) were isolated using an additional DGU iteration targeted to remove residual metallic SWNTs. This separation employed a 3:2 SDS/SC gradient nearly identical to that used for the final s-DWNT iteration. Absorbance spectra from this separation reveal enhancement in the M11 absorption strength coupled with a reduction in S22 intensity (Figure 1f). Moreover, this treatment resulted in a ~20% reduction in background absorption from the elimination of metallic SWNTs.

For SWNT samples, optical absorbance measurements in aqueous solution are routinely used to determine the percentage of semiconducting or metallic species present in sorted samples.[18] This analysis involves integration of the area associated with semiconducting S22 and metallic M11 transitions in absorbance and comparison to an unsorted SWNT sample having a statistical 2:1 ratio of semiconducting to metallic chiralities. Assessment of the outer-wall electronic type purity of DWNTs in aqueous solution, however, is complicated by the overlapping optical transitions arising from the inner and outer DWNT walls. In particular, substantial overlap exists between the M11 (S22) transitions of the outer walls and the S22 (S11) transitions of the inner walls. The S11 excitations of the DWNT outer walls, which do not overlap with any inner-wall excitations, cannot easily be measured in aqueous solution due to the strong absorption of water in this wavelength range.

As a result of the above factors, the semiconducting purity of the DWNT samples was assessed using thin film absorbance measurements. The sorted DWNTs and control samples of unsorted arc discharge SWNTs were processed into semitransparent thin films using vacuum filtration, transferred to glass substrates, and characterized without any high temperature annealing treatment (see Supporting Information for transparent conductor measurements).[21] Use of glass substrates enabled the absorbance of the samples to be measured beyond 2400 nm, a range sufficient to detect S11 absorption from the largest diameter DWNT outer walls (Figure 2, solid curves). The thin film absorption spectra of the s-DWNTs and m-DWNTs both provide further evidence of enrichment by electronic type. The S11 absorption peaks of the outer walls of the m-DWNTs are almost completely eliminated compared to those of the s-DWNT outer walls. The S11 absorption peak of the s-DWNTs also appears relatively weak compared to that measured for the arc discharge SWNTs. This effect is due to the overlap of the S22 outer wall and S11 inner-wall absorption features, which increase overall s-DWNT absorption from *ca.* 850−1350 nm, and the normalization protocol applied to the absorbance spectra (see Methods). All three samples were then treated[6] with thionyl chloride, a common p-type dopant of carbon nanotubes.[6,22] The shifting of the Fermi level induced by doping strongly modifies the optical absorption of the DWNT outer walls (Figure 2, dashed curves). The S11 and S22 transitions of the DWNT outer walls and the SWNTs are completely eliminated or strongly suppressed. As observed previously for highly enriched DWNTs, the transitions associated with the DWNT inner walls are not as significantly attenuated by doping as a result of the chemical and electronic screening effect of the DWNT outer wall. Consequently, comparison of the film absorbance before and after exposure to thionyl

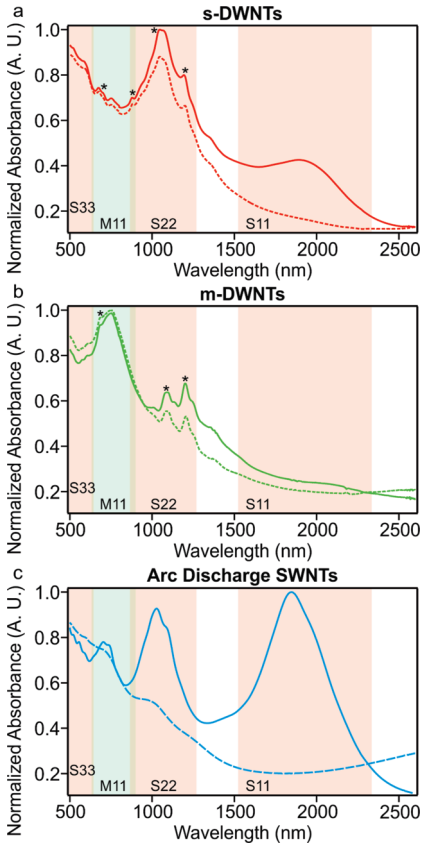


**Figure 2. Optical absorbance of semitransparent thin films of (a) s-DWNTs, (b) m-DWNTs, and (c) unsorted arc discharge SWNTs. Measurements on pristine and thionyl chloride doped films are shown by solid and dashed lines, respectively. Asterisks mark absorption peaks attributed to DWNT inner walls.**

chloride enables identification of excitations arising from the DWNT inner walls. The absorption peaks attributed to the DWNT inner walls are marked by asterisks in Figure 2.

The electronic type purity of the sorted DWNTs can be determined after measurements of the absorption from the outer-wall S11 and M11 transitions and identification of peaks arising from the inner walls. For this calculation, the area under the S11 and M11 peaks was calculated by integration in energy-space after background and inner-wall peak subtraction. Comparison of these integrated areas with those measured for arc discharge SWNTs having a known 2:1 semiconductor to metal ratio yields the purity levels of the sorted DWNTs. This analysis indicates outer-wall purities of 96% for s-DWNTs and 98% for the m-DWNTs.

Raman spectroscopy was used to assess the diameter distributions of the DWNTs and determine the extent of any electronic type enrichment of the inner walls. Thin films of s-DWNTs and m-DWNTs were probed using two laser lines: a 514.5 nm excitation in resonance with metallic inner walls and semiconducting outer walls, and a 750 nm excitation in resonance with semiconducting inner walls and metallic outer

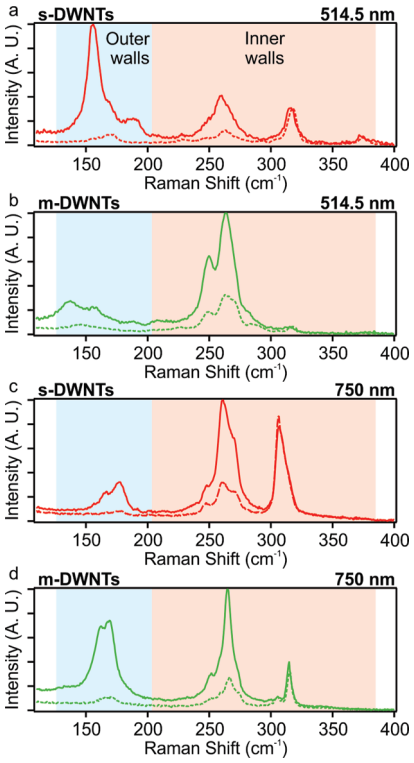


**Figure 3. Raman spectroscopy of thin films of s-DWNTs and m-DWNTs at excitation wavelengths of 514.5 and 750 nm. Spectra obtained from pristine and $H_2SO_4$-treated films are shown with solid and dashed lines, respectively. RBMs associated with the inner and outer walls of the DWNTs are shaded red and blue, respectively. Inner and outer-wall boundaries were determined on the basis of the observed RBM frequencies and the expected ~0.68 nm difference between inner and outer-wall diameters. The maximum RBM peak in each pristine DWNT spectrum is normalized to the same intensity in all the panels. The spectra of the doped DWNT samples are scaled by the same factor used to normalize the corresponding pristine spectrum.**

walls. Raman spectra obtained from the radial breathing mode (RBM) region are presented in Figure 3. The diameters of carbon nanotubes are related to their RBM frequencies $\omega_{RBM,}$ using the equation $\omega_{RBM} = 218.2/d_t + 19.6$ cm$^{-1}$, where $d_t$ is the diameter of the nanotubes specified in nanometers and the formula constants were determined from measurements on thin films of solution-processed SWNTs.[6] Accordingly, the RBM peaks in Figure 3 can be unambiguously assigned to either the inner or outer walls of the DWNTs. For the inner-wall species, RBMs are observed under all four sample/excitation conditions. Since both inner-wall semiconducting and metallic species are in resonance under these conditions, this observation demonstrates the inner DWNT walls are not substantially enriched in a particular electronic type following DGU processing. The diameter of the inner walls of both sorted DWNT materials was found to be ~0.86 nm on average, in agreement with previous measurements on DGU-processed DWNTs.[6]

Comparison of the RBM intensity of the outer walls yields further evidence of enrichment by outer-wall electronic type. For s-DWNTs, excitation at 514.5 nm efficiently excites the majority semiconducting outer-wall RBMs, while a considerably weaker signal is observed for the 750 nm excitation tuned to minority metallic outer-wall species. As expected, the inverse effect is detected in m-DWNTs. In addition, a sizable shift in the outer-wall RBMs of both DWNT samples is observed for the two excitation wavelengths. For the s-DWNTs, the majority species excited at 514.5 nm have a mean diameter of ~1.54 nm while the minority species at 750 nm have a smaller mean diameter of ~1.42 nm. Similarly, the majority m-DWNT species at 750 nm excitation have a mean diameter of ~1.50 nm compared to the larger diameter ~1.71 nm species observed under 514.5 nm illumination. We attribute the outer-wall RBM signal detected from the excitation of minority species to two sources. In agreement with absorption measurements, some of the RBM signal is due to impurity DWNTs of the opposite electronic type. In addition, DWNTs possessing the majority outer-wall electronic type and with diameters at the extremes of the diameter distribution also contribute to the RBM peaks. For s-DWNTs, the S22 transitions of smaller diameter semiconducting carbon nanotubes are in resonance with the 750 nm laser,[23] and for m-DWNTs, the M22 transitions of larger diameter metallic carbon nanotubes are in resonance with the 514.5 nm laser.[18]

Raman spectroscopy was also performed on the sorted DWNT films after treatment[6] in $H_2SO_4$, a stronger dopant than thionyl chloride, to ensure that the RBM peaks arising from small diameter carbon nanotubes were associated with the inner walls of DWNTs and not impurity SWNTs. Previous studies of $H_2SO_4$-treated DWNTs[24] and *in situ* Raman spectroelectrochemistry measurements[25] have demonstrated that the presence of the DWNT outer wall can decrease the efficiency of charge transfer to the DWNT inner wall. This effect is manifested as a reduction in the extent of RBM quenching for DWNT inner walls compared to SWNTs of similar diameter that are exposed directly to the dopant. $H_2SO_4$ was chosen as the dopant since previous measurements of small diameter SWNTs having a similar diameter distribution to the DWNT inner walls demonstrated nearly complete quenching of RBM peaks after exposure to the acid.[6] Following doping, all samples showed nearly complete suppression of outer-wall RBMs as shown by the dashed curves in Figure 3. In contrast, the ~1.0 nm diameter inner walls retained at least 20% of their initial RBM intensity after doping. For small diameter species with RBMs beyond 300 cm$^{-1}$, the $H_2SO_4$ has little effect on their RBM intensity. As the signal from metallic inner walls has been shown to be efficiently quenched by doping compared to semiconducting inner walls having significant band gaps,[25] we attribute these high frequency peaks to semiconducting carbon nanotubes with the main candidates being the (6,5), (9,1), (7,3), and (8,3) chiralities.

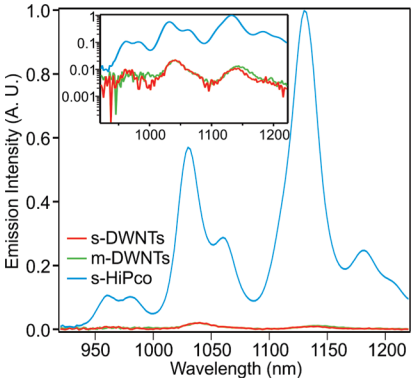


**Figure 4. Photoluminescence spectra of electronic type separated DWNTs *versus* small diameter semiconducting SWNTs excited at 649 nm. All three sorted samples were produced using DGU to ensure similar proportions of individually encapsulated carbon nanotubes, and all samples had similar concentrations. Inset: Photoluminescence spectra plotted on a logarithmic scale. The fluorescence intensity of sorted DWNTs is nearly 2 orders of magnitude lower than semiconducting HiPco SWNTs.**

Photoluminescence measurements were also conducted on solutions containing individually surfactant-encapsulated s-DWNTs and m-DWNTs. In agreement with previous reports on DGU-derived materials,[6,15] only weak fluorescence is detected from these dispersions, most likely as a result of efficient exciton energy transfer to nearby DWNT outer walls having smaller bandgaps.[26] To assess the relative photoluminescence intensity, a control sample consisting of ~0.9 nm mean diameter semiconducting HiPco SWNTs[27] was also measured at a similar concentration to the DWNTs (see Supporting Information). These SWNTs were isolated using a cosurfactant DGU scheme to ensure similar dispersion quality for both the DWNT and SWNT samples. This additional processing *via* DGU was required for valid comparisons since the quantum yield of SWNT dispersions has been shown to improve substantially upon isopycnic fractionation.[28] Figure 4 contains the near-infrared fluorescence detected for the three sorted samples at an excitation wavelength of 649 nm in resonance with both the (7,5) and (7,6) SWNT chiralities. This wavelength was selected since it produced the strongest fluorescence intensity from the DWNT samples. Even at this wavelength, the photoluminescence signal from the DWNTs is almost 2 orders of magnitude lower than that of the semiconducting SWNTs.

The existence of significant photoluminescence from the inner walls of DWNTs has been the subject of conflicting reports in the literature. While previous studies of CVD-grown DWNTs isolated using DGU have demonstrated sharply reduced photoluminescence intensity from small diameter semiconducting carbon nanotubes,[6,15] other reports have noted strong emission from the inner walls of DWNTs.[9,29−31] One such study described the emergence of PL from the inner walls of DWNTs formed by coalescence of $C_{60}$ chains inside nanopeapods.[32] The source of these discrepancies is unclear and suggests that future DGU studies of alternative DWNT starting materials, such as those derived from nanopeapods, are warranted.

The production of SWNTs with predominantly metallic or semiconducting character has facilitated the direct incorporation of SWNTs into thin films with improved electronic properties.[13,18,19,33,34] To directly assess the effects of outer-wall enrichment on the electronic properties of sorted DWNTs, we incorporated 96% pure s-DWNTs and 98% pure m-DWNTs into nanotube network TFTs. In addition, comparison devices composed of 96% pure semiconducting arc discharge SWNTs (s-SWNTs) having similar ~1.5 nm mean diameters were fabricated and characterized.

Submonolayer coverage nanotube networks (Figure 5a) were formed using vacuum filtration[21] and transferred to $SiO_2$-capped silicon wafers bearing predefined Au/Pd electrodes. Devices were measured using a degenerately doped silicon back gate and had a range of channel lengths $L = \{4,8,16,32\}$ $\mu$m with a common channel width $W = 250$ $\mu$m (Figure 5b). Representative $I_{DS}-V_G$ curves with $L = 16$ $\mu$m for the three types of devices are shown in Figure 5c. Although all three devices have similar on currents, their off currents vary by over 3 orders of magnitude with m-DWNTs and s-SWNTs having the largest and smallest off currents, respectively.

To statistically assess these variations in performance, measurements of all three materials were conducted on at least eight different devices for each channel length. The width normalized conductance $G/W$ values compiled from these measurements are shown in Figure 5e. The three types of devices exhibit similar $G/W$ for each channel length, which suggests they all possess comparable nanotube network densities. Device mobilities $\mu_{device}$ were also calculated using the equation:[35]

$$\mu_{device} = \frac{L}{V_{DS}C_{ox}}\frac{g_m}{W}$$

where $g_m$ is the maximum transconductance measured during the forward gate voltage sweep and $C_{ox}$ is the gate capacitance. $C_{ox}$ was calculated using a parallel plate capacitor model and is $3.45 \times 10^{-8}$ F cm$^{-2}$ for the 100 nm thick $SiO_2$ gate dielectric. The mean device mobilities were comparable for the different source materials and ranged from *ca.* 3 to 6 cm$^2$ V$^{-1}$ s$^{-1}$. With similar on currents and mobilities, valid performance comparisons can be made among devices made from the three materials. m-DWNTs display only a weak switching ratio $I_{on}/I_{off}$ of 2−6 under the applied gate bias, which is similar to behavior observed for metallic SWNT thin film FETs.[13] In contrast, the s-DWNTs exhibit average switching ratios over 2 orders of magnitude higher for all values of $L$. The mean

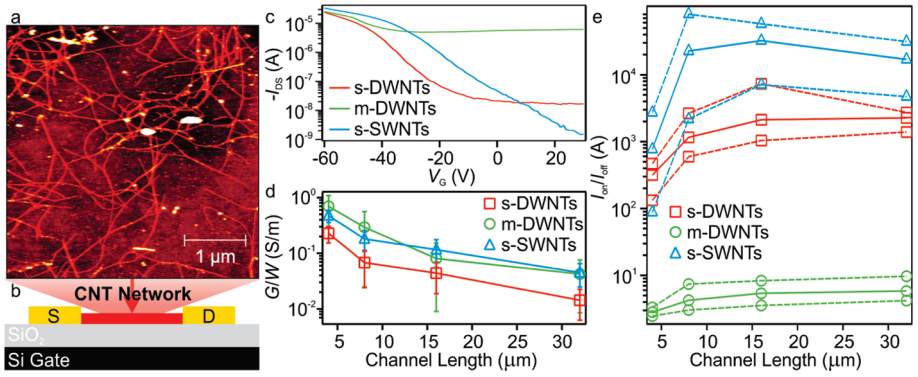


**Figure 5. Characterization of s-DWNT, m-DWNT, and s-SWNT thin film transistors. (a) Atomic force microscope image of the submonolayer s-DWNT network used in the devices. (b) Schematic illustration of TFT geometry. (c) Transfer ($I_{DS}-I_G$) curves of representative s-DWNT, m-DWNT, and s-SWNT devices having $L = 16\ \mu$m at $V_{DS} = -1$ V. (d) Channel width normalized conductance $G/W$ for the three types of devices at different channel lengths. $G/W$ is comparable for the devices and implies they have similar coverage levels. (e) Switching ratio $I_{on}/I_{off}$ for the three types of TFTs as a function of channel length. The solid curves present the mean switching ratios obtained from multiple devices; the dashed lines mark the maximum and minimum switching ratios obtained for a given device geometry. Lines are drawn to aid the eye in panels d and e.**

s-DWNT $I_{on}/I_{off}$ for each value of $L$ progressively increases from ~300 at $L = 4\ \mu$m to ~2300 at $L = 32\ \mu$m. This behavior is expected as the probability of forming a percolating path of metallic DWNTs between the source and drain electrodes decreases as the separation between them increases.

Despite the improved performance of the s-DWNTs, their switching ratios remain an order of magnitude lower than those measured for comparable purity s-SWNTs devices having $L \geq 8\ \mu$m (Figure 5e). We attribute this effect to two factors: additional screening of the gate bias by the DWNT inner walls and modifications of the s-DWNT transport properties caused by interwall interactions. Previous measurements on FETs fabricated from individual large diameter DWNTs have demonstrated distinct $I_{DS}-V_G$ characteristics for devices having different inner and outer-wall electronic type permutations as a result of the above factors.[3,36] In particular, these reports have shown only DWNTs having semiconducting inner and outer walls exhibited switching ratios exceeding 100, while semiconducting outer-wall and metallic inner-wall DWNTs had $I_{on}/I_{off} <$ ~10. Hence, similar effects could be causing higher off currents for these s-DWNT devices. Direct application of the single DWNT transistor measurements to our thin film networks would suggest switching ratios significantly lower than the ones we observe here. This discrepancy is likely due to the smaller outer-wall diameters of the sorted DWNTs (~1.55 nm) compared to those of the previous single DWNT studies (≥2.4 nm).[3,36] The use of smaller diameter DWNTs leads to increased outer-wall band gaps and decreases the strength of interwall electronic coupling.[36] Overall, our s-DWNT-based FETs demonstrate figures of merit sufficient for use in applications such as control[35] and logic[37] circuitry. We expect that further performance improvements can be obtained by using high-k gate dielectrics to minimize nanotube screening effects and with higher purity sorted DWNT materials having inner and outer walls of semiconducting character.

Although the results presented here demonstrate only separation of DWNTs by outer-wall electronic type, the electrical behavior of these sorted DWNTs in TFTs suggests there is weak but still sufficient coupling between inner and outer walls to enable isolation of all four DWNT permutations. For instance, screening by inner metallic walls is likely strong enough to induce minute changes in the encapsulation of DWNTs by surfactants. Such variations can be resolved using a combination of shallower density gradients and longer centrifugation times compared to the ones used here, as suggested by previous studies separating SWNT enantiomers.[38,39] Recent molecular dynamics studies of surfactant interactions with SWNTs have highlighted the possible role of surfactant molecules inside SWNTs during DGU experiments.[40] Extension of this concept to molecules having filling affinity for carbon nanotubes of a particular electronic type could dramatically enhance separations according to the DWNT inner walls. Furthermore, we expect that inner-wall electronic type separations will be improved by using DWNTs with larger diameters, as this should increase electronic coupling between inner and outer walls.

## CONCLUSIONS

DWNTs having highly pure semiconducting or metallic outer walls have been produced using DGU. A multistage separation strategy was used to isolate the double-walled material from single-walled species and to generate DWNTs with semiconducting and metallic outer-wall purities of 96% and 98%, respectively. The enriched DWNT materials were characterized using optical absorbance and Raman spectroscopy to confirm wall number and electronic type enrichment. Photoluminescence measurements of the semiconducting and metallic outer-wall DWNTs reveal weak

emission from both samples and provide evidence of inner-wall fluorescence quenching due to the DWNT outer walls. Lastly, TFTs were fabricated from networks of the sorted DWNTs and semiconducting SWNTs. Comparison of these devices confirms that semiconducting outer-wall DWNTs offer substantial improvements in switching ratio compared to metallic outer-wall DWNTs. However, semiconducting DWNT devices do not perform as well as semiconducting SWNTs likely as a result of gate screening and perturbations to the DWNT electronic structure caused by the inner wall. The results and separation methods presented here should enable future studies of interwall interactions in carbon nanotubes[25] and encourage additional studies of charge transport in sorted DWNT networks.

## METHODS

**Coarse Wall Number Separation of DWNTs.** Starting carbon nanotube material (Purified Double-Wall Carbon Nanotubes from Unidym, Inc., batch number: DW411UA) was first dispersed in 100 mL of 1% w/v SC aqueous solution as described previously.[6] This polydisperse carbon nanotube mixture was separated in iodixanol density gradients homogeneously loaded with 1% w/v SC. A 15 mL linear density gradient ranging from 25% to 40% w/v iodixanol was formed at the bottom of a centrifuge tube using a linear gradient maker (Hoefer SG15) and the dispersion of carbon nanotubes was carefully added on top. The resulting density gradients were centrifuged for 18 h at 32 krpm and 22 °C in an SW 32 Ti rotor (Beckman-Coulter). Following separation, nanotube bands were extracted from the centrifuge tube using a piston gradient fractionator (Biocomp Instruments).

**Isolation of Semiconducting Outer-Wall DWNTs.** Semiconducting outer-wall DWNTs were produced using three iterations of DGU. In the first iteration, coarsely enriched DWNTs were injected below a linear density gradient containing a homogeneous 1% w/v 1:4 SDS/SC surfactant loading. This density gradient was centrifuged at 41 krpm for 14 h at 22 °C using an SW 41 Ti rotor (Beckman-Coulter). Following piston gradient fractionation, semiconducting DWNT fractions were diluted by a factor of approximately three into 1% w/v SC aqueous solution for optical absorbance spectroscopy. The highest purity semiconducting DWNTs from this stage were directly incorporated into a second separation loaded with 1% w/v 1:4 SDS/SC with the nanotubes initially positioned at the top of the linear density gradient. After separation and optical characterization, the remaining metallic carbon nanotubes were removed from the second iteration semiconducting DWNTs using a final DGU separation in 1% w/v 3:2 SDS/SC. Full DGU parameters including gradient densities, layer volumes, centrifugation times, and rotors are presented in Table S-1 of the Supporting Information.

**Isolation of Metallic Outer-Wall DWNTs.** Metallic outer-wall DWNTs were produced using two iterations of DGU. In the first iteration, coarsely enriched DWNTs were infused below a linear density gradient containing 1% w/v 3:2 SDS/SC. This density gradient was centrifuged at 41 krpm for 14 h at 22 °C using an SW 41 Ti rotor. After fractionation, the resulting material was diluted with 1% w/v 3:2 SDS/SC aqueous solution for optical characterization. The highest purity metallic DWNTs were then sorted using a density gradient containing 1% w/v 3:2 SDS/SC with the nanotubes loaded at the top of the linear density gradient region. Full DGU parameters including gradient densities, layer volumes, centrifugation times, and rotors are presented in Table S-2 of the Supporting Information.

**Carbon Nanotube Network TFT Preparation and Characterization.** Percolating carbon nanotube networks were prepared using vacuum filtration.[21] Controlled volumes of sorted carbon nanotube solution were filtered through mixed cellulose ester (MCE) membranes (50 nm pore size, Millipore), and copiously rinsed with deionized water to remove any residual surfactants and iodixanol from the nanotube network.

Electrode arrays were prepared on degenerately doped silicon wafers with a 100 nm thick dry thermal oxide layer (Silicon Quest International) using photolithographic processing. An Au/Pd layer, approximately 30 nm thick, was deposited onto the wafers followed by lift off to complete electrode fabrication.

Nanotube networks on MCE were transferred to the patterned wafers by placing them in direct contact with the predefined electrode arrays and exposing them to an acetone vapor bath, which initiated dissolution of the MCE membrane. Three consecutive acetone liquid baths of at least 15 min each were employed to complete dissolution of the filter membrane, followed by a 15 min rinsing step in an ethanol liquid bath. The devices were then annealed in air at 225 °C for 20 min to remove residual MCE and to improve nanotube−metal contacts. TFTs were characterized with a Cascade Microtech M150 probe station in ambient conditions using a pair of Keithley model 2400 digital source meters.

**Normalization of Optical Absorbance and Raman Spectra.** Normalized absorbance spectra were obtained by scaling experimental absorbance spectra to ensure their maximum absorbance values were equal to 1 over the plotted wavelength range. For doped thin film samples in Figure 2, the absorbance normalization factor was calculated from measurements of the pristine film and applied to the spectrum obtained from the film after doping. An analogous normalization procedure was used for Raman spectroscopy of pristine and doped DWNT thin films as shown in Figure 3.

**AFM Imaging.** AFM images of the percolating carbon nanotube network were obtained using a Thermo Microscopes Autoprobe CP-Research AFM. Images were acquired in tapping mode using conical AFM tips (MikroMasch, NSC36/Cr−Au BS).

*Acknowledgment.* This work was supported by the National Science Foundation (DMR-0520513, EEC-0647560, DMR-0706067, and DMR-1006391), the Office of Naval Research (N00014-09-1-0180 and N00014-09-1-0795), and the Nanoelectronics Research Initiative. A Natural Sciences and Engineering Research Council of Canada Postgraduate Scholarship (A.A.G.) is also acknowledged. This research utilized instruments in the Keck-II facility of the NUANCE Center at Northwestern University, the Keck Biophysics Facility at Northwestern University, and the Center for Nanoscale Materials at Argonne National Laboratory. The Center for Nanoscale Materials is supported by the U.S. Department of Energy, Office of Science, Office of Basic Energy Sciences, under Contract No. DE-AC02-06CH11357. We thank R. Divan and V. Sangwan for assistance with photolithography.

*Supporting Information Available:* Full DGU parameters including gradient densities, layer volumes, centrifugation times, and rotors; DWNT Kataura plot; additional absorbance spectra; transparent conductor measurements. This material is available free of charge *via* the Internet at http://pubs.acs.org.

## REFERENCES AND NOTES

1. Shimada, T.; Sugai, T.; Ohno, Y.; Kishimoto, S.; Mizutani, T.; Yoshida, H.; Okazaki, T.; Shinohara, H. Double-Wall Carbon Nanotube Field-Effect Transistors: Ambipolar Transport Characteristics. *Appl. Phys. Lett.* **2004,** *84*, 2412–2414.
2. Li, Y. F.; Hatakeyama, R.; Kaneko, T.; Izumida, T.; Okada, T.; Kato, T. Electronic Transport Properties of Cs-Encapsulated Double-Walled Carbon Nanotubes. *Appl. Phys. Lett.* **2006,** *89*, 093110.

3. Liu, K.; Wang, W.; Xu, Z.; Bai, X.; Wang, E.; Yao, Y.; Zhang, J.; Liu, Z. Chirality-Dependent Transport Properties of Double-Walled Nanotubes Measured *in Situ* on Their Field-Effect Transistors. *J. Am. Chem. Soc.* **2008,** *131*, 62–63.
4. Qian, H.; Araujo, P. T.; Georgi, C.; Gokus, T.; Hartmann, N.; Green, A. A.; Jorio, A.; Hersam, M. C.; Novotny, L.; Hartschuh, A. Visualizing the Local Optical Response of Semiconducting Carbon Nanotubes to DNA-Wrapping. *Nano Lett.* **2008,** *8*, 2706–2711.
5. Brozena, A. H.; Moskowitz, J.; Shao, B. Y.; Deng, S. L.; Liao, H. W.; Gaskell, K. J.; Wang, Y. H. Outer Wall Selectively Oxidized, Water-Soluble Double-Walled Carbon Nanotubes. *J. Am. Chem. Soc.* **2010,** *132*, 3932–3938.
6. Green, A. A.; Hersam, M. C. Processing and Properties of Highly Enriched Double-Wall Carbon Nanotubes. *Nat. Nanotechnol.* **2009,** *4*, 64–70.
7. Sugai, T.; Yoshida, H.; Shimada, T.; Okazaki, T.; Shinohara, H. New Synthesis of High-Quality Double-Walled Carbon Nanotubes by High-Temperature Pulsed Arc Discharge. *Nano Lett.* **2003,** *3*, 769–773.
8. Lyu, S. C.; Lee, T. J.; Yang, C. W.; Lee, C. J. Synthesis and Characterization of High-Quality Double-Walled Carbon Nanotubes by Catalytic Decomposition of Alcohol. *Chem. Commun.* **2003,** 1404–1405.
9. Kishi, N.; Kikuchi, S.; Ramesh, P.; Sugai, T.; Watanabe, Y.; Shinohara, H. Enhanced Photoluminescence from Very Thin Double-Wall Carbon Nanotubes Synthesized by the Zeolite-CCVD Method. *J. Phys. Chem. B* **2006,** *110*, 24816–24821.
10. Yamada, T.; Namai, T.; Hata, K.; Futaba, D. N.; Mizuno, K.; Fan, J.; Yudasaka, M.; Yumura, M.; Iijima, S. Size-Selective Growth of Double-Walled Carbon Nanotube Forests from Engineered Iron Catalysts. *Nat. Nanotechnol.* **2006,** *1*, 131–136.
11. Hersam, M. C. Progress Towards Monodisperse Single-Walled Carbon Nanotubes. *Nat. Nanotechnol.* **2008,** *3*, 387–394.
12. Green, A. A.; Hersam, M. C. Ultracentrifugation of Single-Walled Nanotubes. *Mater. Today* **2007,** *10*, 59–60.
13. Arnold, M. S.; Green, A. A.; Hulvat, J. F.; Stupp, S. I.; Hersam, M. C. Sorting Carbon Nanotubes by Electronic Structure Using Density Differentiation. *Nat. Nanotechnol.* **2006,** *1*, 60–65.
14. Green, A. A.; Hersam, M. C. Solution Phase Production of Graphene with Controlled Thickness *via* Density Differentiation. *Nano Lett.* **2009,** *9*, 4031–4036.
15. Tsyboulski, D. A.; Hou, Y.; Fakhri, N.; Ghosh, S.; Zhang, R.; Bachilo, S. M.; Pasquali, M.; Chen, L. W.; Liu, J.; Weisman, R. B. Do Inner Shells of Double-Walled Carbon Nanotubes Fluoresce? *Nano Lett.* **2009,** *9*, 3282–3289.
16. Fleurier, R.; Lauret, J. S.; Flahaut, E.; Loiseau, A. Sorting and Transmission Electron Microscopy Analysis of Single or Double Wall Carbon Nanotubes. *Phys. Status Solidi B* **2009,** *246*, 2675–2678.
17. Huh, J. Y.; Walker, A. R. F.; Ro, H. W.; Obrzut, J.; Mansfield, E.; Geiss, R.; Fagan, J. A. Separation and Characterization of Double-Wall Carbon Nanotube Subpopulations. *J. Phys. Chem. C* **2010,** *114*, 11343–11351.
18. Green, A. A.; Hersam, M. C. Colored Semitransparent Conductive Coatings Consisting of Monodisperse Metallic Single-Walled Carbon Nanotubes. *Nano Lett.* **2008,** *8*, 1417–1422.
19. Engel, M.; Small, J. P.; Steiner, M.; Freitag, M.; Green, A. A.; Hersam, M. C.; Avouris, P. Thin Film Nanotube Transistors Based on Self-Assembled, Aligned, Semiconducting Carbon Nanotube Arrays. *ACS Nano* **2008,** *2*, 2445–2452.
20. Sun, X.; Zaric, S.; Daranciang, D.; Welsher, K.; Lu, Y.; Li, X.; Dai, H. Optical Properties of Ultrashort Semiconducting Single-Walled Carbon Nanotube Capsules Down to Sub-10 nm. *J. Am. Chem. Soc.* **2008,** *130*, 6551–6555.
21. Wu, Z. C.; Chen, Z. H.; Du, X.; Logan, J. M.; Sippel, J.; Nikolou, M.; Kamaras, K.; Reynolds, J. R.; Tanner, D. B.; Hebard, A. F.; *et al.*Transparent, Conductive Carbon Nanotube Films. *Science* **2004,** *305*, 1273–1276.
22. Dettlaff-Weglikowska, U.; Skakalova, V.; Graupner, R.; Jhang, S. H.; Kim, B. H.; Lee, H. J.; Ley, L.; Park, Y. W.; Berber, S.; Tomanek, D.; *et al.*Effect of $SOCl_2$ Treatment on Electrical and Mechanical Properties of Single-Wall Carbon Nanotube Networks. *J. Am. Chem. Soc.* **2005,** *127*, 5125–5131.
23. Weisman, R. B.; Bachilo, S. M. Dependence of Optical Transition Energies on Structure for Single-Walled Carbon Nanotubes in Aqueous Suspension: An Empirical Kataura Plot. *Nano Lett.* **2003,** *3*, 1235–1238.
24. Barros, E. B.; Son, H.; Samsonidze, G. G.; Souza, A. G.; Saito, R.; Kim, Y. A.; Muramatsu, H.; Hayashi, T.; Endo, M.; Kong, J.; *et al.*Raman Spectroscopy of Double-Walled Carbon Nanotubes Treated with $H_2SO_4$. *Phys. Rev. B* **2007,** *76*, 045425.
25. Kalbac, M.; Green, A. A.; Hersam, M. C.; Kavan, L. Tuning of Sorted Double-Walled Carbon Nanotubes by Electrochemical Charging. *ACS Nano* **2010,** *4*, 459–469.
26. Qian, H. H.; Georgi, C.; Anderson, N.; Green, A. A.; Hersam, M. C.; Novotny, L.; Hartschuh, A. Exciton Energy Transfer in Pairs of Single-Walled Carbon Nanotubes. *Nano Lett.* **2008,** *8*, 1363–1367.
27. Naumov, A. V.; Kuznetsov, O. A.; Harutyunyan, A. R.; Green, A. A.; Hersam, M. C.; Resasco, D. E.; Nikolaev, P. N.; Weisman, R. B. Quantifying the Semiconducting Fraction in Single-Walled Carbon Nanotube Samples through Comparative Atomic Force and Photoluminescence Microscopies. *Nano Lett.* **2009,** *9*, 3203–3208.
28. Crochet, J.; Clemens, M.; Hertel, T. Quantum Yield Heterogeneities of Aqueous Single-Wall Carbon Nanotube Suspensions. *J. Am. Chem. Soc.* **2007,** *129*, 8058–8059.
29. Hertel, T.; Hagen, A.; Talalaev, V.; Arnold, K.; Hennrich, F.; Kappes, M.; Rosenthal, S.; McBride, J.; Ulbricht, H.; Flahaut, E. Spectroscopy of Single- and Double-Wall Carbon Nanotubes in Different Environments. *Nano Lett.* **2005,** *5*, 511–514.
30. Iakoubovskii, K.; Minami, N.; Kazaoui, S.; Ueno, T.; Miyata, Y.; Yanagi, K.; Kataura, H.; Ohshima, S.; Saito, T. IR-Extended Photoluminescence Mapping of Single-Wall and Double-Wall Carbon Nanotubes. *J. Phys. Chem. B* **2006,** *110*, 17420–17424.
31. Iakoubovskii, K.; Minami, N.; Ueno, T.; Kazaoui, S.; Kataura, H. Optical Characterization of Double-Wall Carbon Nanotubes: Evidence for Inner Tube Shielding. *J. Phys. Chem. C* **2008,** *112*, 11194–11198.
32. Muramatsu, H.; Hayashi, T.; Kim, Y. A.; Shimamoto, D.; Endo, M.; Meunier, V.; Sumpter, B. G.; Terrones, M.; Dresselhaus, M. S. Bright Photoluminescence from the Inner Tubes of "Peapod"-Derived Double-Walled Carbon Nanotubes. *Small* **2009,** *5*, 2678–2682.
33. Nougaret, L.; Happy, H.; Dambrine, G.; Derycke, V.; Bourgoin, J. P.; Green, A. A.; Hersam, M. C. 80 Ghz Field-Effect Transistors Produced Using High Purity Semiconducting Single-Walled Carbon Nanotubes. *Appl. Phys. Lett.* **2009,** *94*, 243505.
34. Ha, M.; Xia, Y.; Green, A. A.; Zhang, W.; Renn, M. J.; Kim, C. H.; Hersam, M. C.; Frisbie, C. D. Printed, Sub-3V Digital Circuits on Plastic from Aqueous Carbon Nanotube Inks. *ACS Nano* **2010,** *4*, 4388−4395.
35. Wang, C.; Zhang, J.; Ryu, K.; Badmaev, A.; De Arco, L. G.; Zhou, C. Wafer-Scale Fabrication of Separated Carbon Nanotube Thin-Film Transistors for Display Applications. *Nano Lett.* **2009,** *9*, 4285–4291.
36. Wang, S.; Liang, X. L.; Chen, Q.; Zhang, Z. Y.; Peng, L. M. Field-Effect Characteristics and Screening in Double-Walled Carbon Nanotube Field-Effect Transistors. *J. Phys. Chem. B* **2005,** *109*, 17361–17365.
37. Cao, Q.; Kim, H. S.; Pimparkar, N.; Kulkarni, J. P.; Wang, C. J.; Shim, M.; Roy, K.; Alam, M. A.; Rogers, J. A. Medium-Scale Carbon Nanotube Thin-Film Integrated Circuits on Flexible Plastic Substrates. *Nature* **2008,** *454*, 495–500.
38. Green, A. A.; Duch, M. C.; Hersam, M. C. Isolation of Single-Walled Carbon Nanotube Enantiomers by Density Differentiation. *Nano Res.* **2009,** *2*, 69–77.
39. Ghosh, S.; Bachilo, S. M.; Weisman, R. B. Advanced Sorting of Single-Walled Carbon Nanotubes by Nonlinear Density-Gradient Ultracentrifugation. *Nat. Nanotechnol.* **2010,** *5*, 443–450.
40. Carvalho, E. J. F.; dos Santos, M. C. Role of Surfactants in Carbon Nanotubes Density Gradient Separation. *ACS Nano* **2010,** *4*, 765–770.